2021 18th International Conference on Electrical Engineering, Computing Science and Automatic Control (CCE). Mexico City, Mexico. November 10-12, 2021

Temperature prediction based on ANN linear regression with an LWIR sensor for the study of diabetic foot

Rafael Bayareh Mancilla
Department of Electrical Engineering/Bioelectronics, CINVESTAV-IPN
Université de Lorraine - CRAN-BioSiS
Mexico City, Mexico - Nancy, France
rafael.bayareh@cinvestav.mx

Christian Daul
Université de Lorraine/CNRS, CRAN-BioSiS
Nancy, France

Josefina Gutierrez Martínez
INR-LGII, Direction of Technological Research, Medical Engineering Research Division
Mexico City, Mexico

Lorenzo Leija Salas
Department of Electrical Engineering/Bioelectronics, CINVESTAV-IPN
Mexico City, Mexico
lleija@cinvestav.mx Didier Wolf

Université de Lorraine/CNRS, CRAN
Nancy, France
didier.wolf@univ-lorraine.fr

Arturo Vera Hernández
Department of Electrical Engineering/Bioelectronics, CINVESTAV-IPN
Mexico City, Mexico
arvera@cinvestav.mx

Abstract — **This work presents an improvement to a linear model obtained by Bayareh et al. in 2017, by training a single layer Perceptronand optimized by Gradient Descent. The objective of characterizing an IR radiometric sensor with a mathematical model is to predict the surface temperature of the body under study (e.g. diabetic foot) to perform quantitative thermography studies related to early detection through temperature difference. The data was obtained by measuring IR radiometric information on a phantom under a controlled environment. Subsequently, the predicted model was compared to the first characteristic equation. The model had an error of 0.14°C while the original model had an error of 1.28ºC regard an industrial purpose camera, previously calibrated.. The updated model could support the study of quantitative thermography with embedded systems whose sensors are not able to interpret temperature from factory settings, especially in studies focused on the difference of temperatures that support the diagnosis from the quantitative point of view.**

Keywords —IR medical thermography, Artificial Neural Network, Diabetic foot.

I. INTRODUCTION

The International Diabetes Federation has reported four million diseases each year due to Diabetes Mellitus (DM), which other millions more have medical complications, e.g. diabetic foot (DF) [1]. DF is considered a complication towards disabling due to lower limb amputation as a consequence of neuropathy, vascular insufficiency, infectious process, or a combination of these factors [2,3]. Early identification and medical therapy of the DF could avoid several surgical interventions, the most common is the amputation below the knee joint as a preventive measure [4]. Infrared thermography (IRT), contactless and non-invasive technology for superficial temperature detection, is a revolutionary and modern method for medical support and diagnosis. [5–7]. The asymmetric temperature is a strong indicator of any pathology [8]. However, IRT is not a standardized approach that can't be widely acknowledged as a method of diagnosing without medical criteria.. The importance of quantification of clinical data is relevant to the understanding of the nature of thermal imaging, training, and interpretation [6].

IRT is based on the indirect measurement of the IR energy emitted by a body containing the minimum amount of heat, whose temperature is greater than absolute zero. The radiometric data is interpreted on temperature scales after data processing (i.e. IR radiometric processing). The results obtained from radiometric processing are generally interpreted as false-color images known as thermographic images. Recent developments in the production of electronic display chips enable the achievement of higher resolution thermographic images, which main advantage is real-time temperature measurement with relatively low-cost devices [9,10]. However, several low-cost technologies, usually, are not calibrated neither are capable of adjusting thermal parameters depending on the measured materials [11]. IR measurements are sensitive to environmental variations such as ambient temperature, relative humidity, and air flows [12]. Also, thermal backgrounds interferences may affect directly the representation of false-color images.

The latter described factors, are not contemplated in this type of low-cost sensor. Therefore, performing calibration in a controlled environment that is dependent on the material emissivity is critical.. Thermal calibrations are carried out with a blackbody. Manufactures offer black bodies with a coating material as close as possible to perfect emissivity. According to Plank's Law, a blackbody is an object that absorbs IR radiation, considered as an object with emissivity = 1 [13]. However, human skin emissivity is reported to be approximately 0.98 [14]. Thus, employing a homemade blackbody is common practice with a value of approximately 0.98, similar to human skin emissivity [15–17].

Temperature prediction by radiometric data processing has typically a linear nature, under a controlled environment [18,19]. The aim of an Artificial Neural Network (ANN) is to predict events or classifications being the simplest model a linear prediction without an activation function.This work

978-1-6654-0029-9/21/$31.00 ©2021 IEEE

presents an improvement to the temperature prediction through the linear regression with Perceptron method and Gradient descent optimization of the Long-Wave Infrared (LWIR) Lepton 2.5 sensor reported in [15]. The manuscript is detailed as follows. Section II describes the methodology background regarding thermal calibration, radiometric data processing with an ANN, and validation. Section III details the results of the comparison between both characterizations and the error regarding an industrial thermal camera previously calibrated. Finally, sections IV and V discuss and conclude the implementation of an ANN to obtain a linear model that predicts temperature from radiometric data for the study of the diabetic foot through temperature differences.

II. METHODS

A. *Instrumentation features*

The data was retrieved with a low-cost (one-tenth the cost of traditional IR cameras according to the developers) development sensor kit Lepton 2.5 (Flir, OR, USA) for general purposes (Fig. 1). Lepton can be integrated into mobile technology such as portable prototypes as an IR sensor or thermal imager, as reported in [11]. Table 1 summarizes the thermal imager technical characteristics.

Table 1: Lepton 2.5 LWIR thermal imager

Characteristics	Range	Units
IR sensor resolution	80 x 60	Pixel
Pixel size	17	µm
Thermal Sensitivity	≤ 50	mK
Infrared Spectral Band	8 – 14	µm
Voltage	2.8	V
Refresh rate	8.6	FPS

The retrieved information is a matrix with double type values, containing 14-bits data elements. Each matrix was obtained by a single capture during the thermal calibration, detailed in the next subsection.

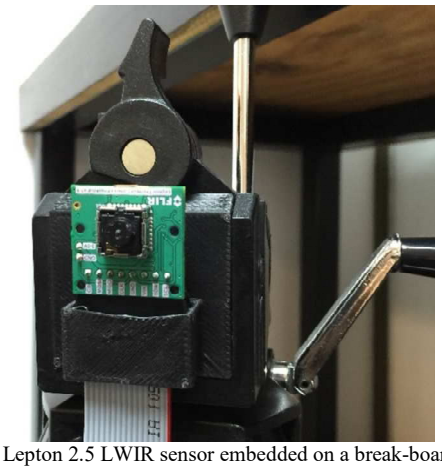

Fig. 1: Lepton 2.5 LWIR sensor embedded on a break-board.

B. *Thermal Calibration*

The objective of the thermal calibration was to obtain radiometric information with the Lepton sensor and thermal maps (in Celsius scale) with the Ti32 thermal camera (Fluke, Everett, WA, USA). The Ti32 equipment was previously calibrated with a gold standard thermometer. In this way, the radiometric information would be compared against each value obtained by the thermal camera.

The calibration was performed with a black body (phantom). The phantom was a10 cm x 10 cm aluminum plate painted black with a matte texture. The phantom was placed on a thermo-static bath, illustrated in Fig. 2. The sensor and the thermal camera were placed 20 cm from the phantom. The emissivity of the thermal camera was set to 0.98 (resembling the emissivity of the skin).

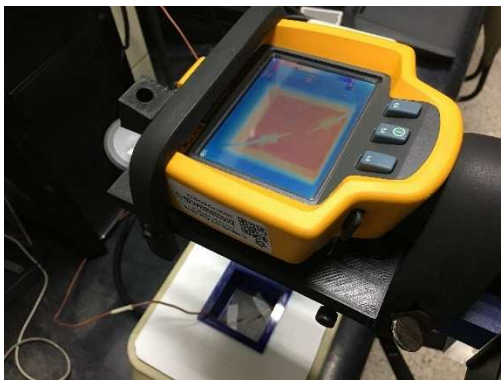

Fig. 2: Thermal phantom inside the thermostatic water bath. The setup ensured a controlled environment, in which the temperature and humidity were controlled, and air flows were avoided.

The thermal bath was set from 22°C to 44°C in 2°C steps and a phantom stabilization time of 2 min.

C. *Data analysis*

The IR data and the superficial temperature were measured on the surface of the phantom with a homogeneous distribution (Fig. 3). The dataset consisted of 948 different values, in which each vector was paired regard the warmest spot (i.e. the highest temperature was paired with the highest raw value). IRT radiometric data and IR images take as reference the warmest point inside the capture frame. This feature may lead to thermal artifacts if the environment is not controlled in the acquisition protocol stage, as reported in [20]. The temperature data were obtained from the IS2 files using a modified version of the code presented by Beauducel in [21], while the radiometric data were extracted with the code presented in [22]. The temperature matrices were considered as the target data while the radiometric information would be the input data to the training system. When comparing the set of data pairs, a linear nature was observed (Fig. 4), therefore, the only adjustable solution to the problem would be a linear regression (the simplest solution of an ANN).

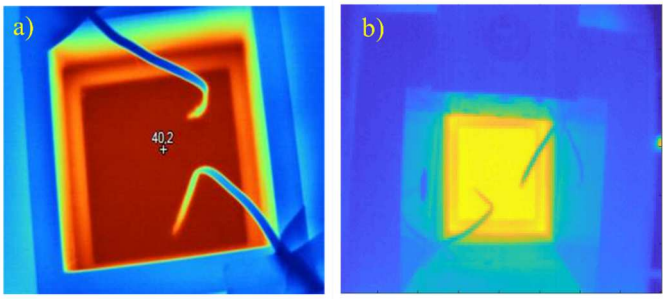

Fig. 3: a) IR images of the phantom inside the thermal bath. a) Sample taken with the Ti32 thermal camera, b) sample taken with Lepton 2.5 LWIR sensor.

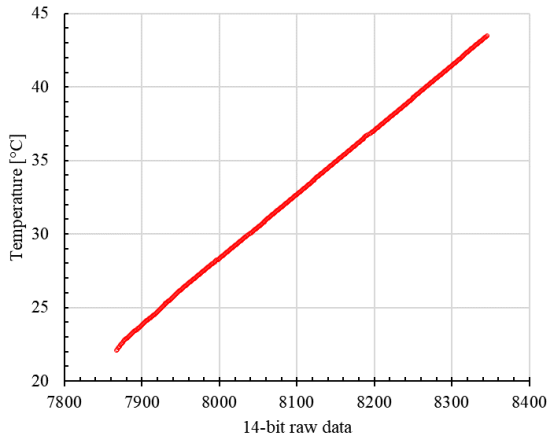

Fig. 4: Data-pair of temperature recorded by the Ti32 thermal camera and the Lepton 2.5 radiometric data on a 14-bit scale. Although a continuous straight line is observed, it is a series of 948 individual points.

The proposed ANN is a single layer for the input and a single layer for the output, as a configuration for model linear responses [23]. Linear regression is considered an approach in this work due to the simplicity and nature of the retrieved data. Neural Networks are increasing acceptance for several tasks, such as prediction or classification [24]. The purpose is to fit a mathematical model describing a curve among several data points. The mathematical model will predict (interpolate) a result regarding a set of known values. The simplest model to design the ANN algorithm is known as Perceptron. It is inspired by the functioning of biological neurons and was proposed in 1957 by F. Rosenblatt [25]. The model proposed is described in Fig. 5. The Perceptron is the basic computing unit used in neural networks, although it can also be used on its own as an AI algorithm in some cases.

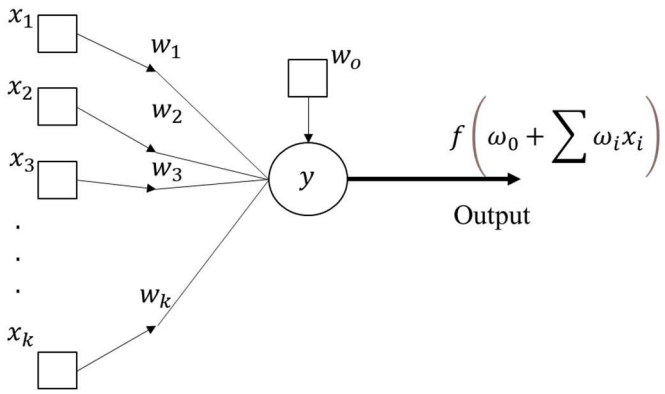

Fig. 5: Single layer Perceptron model without activation function. The output y_k is a multiplicative factor summed with a bias that predicts the temperature as a function of the lepton sensor values.

The Perceptron is a simplified version of a neuron that computes the weighted sum of all its inputs and then applies an activation function to give the result (equation 1).

$$y = \omega_0 + \sum_{i=1}^{k} \omega_i x_i \tag{1}$$

where the inputs $x_1 \dots x_n$ are the raw data retrieved from the Lepton sensor, ω_i is the computed weights (multiplicative factor), ω_0 is the bias and y is the output linear prediction.

Despite the fact that the Perceptron model has an activation function for classification, it was not considered for this project since the goal is to obtain an equation that predicts temperature based on the sensor's radiometric data. For this type of regression problem, it is pursued a model that best fits a given data set in which the Perceptron model will be a straight line resembling the linear nature of the data set (see Fig. 4), described as a gradient line in equation 2.

$$y = w \cdot x + b \tag{2}$$

In order to evaluate the performance, it is necessary to determine if the model predicts the target with relatively acceptable accuracy. The objective is to find weights and a bias of the model in equation 2, that minimize a loss function. This data is useful for computing the error of the model. In regression methods, the most commonly used loss function is the Mean Squared Error (MSE), described in equation 3 [24].

$$MSE(\hat{y}, y) = \frac{1}{N}\sum_{j=1}^{N}(\hat{y}_j - y_j)^2 \tag{3}$$

where N es the number of the dataset, $\hat{y}_j$ is the prediction computed regarding the dataset, and y_j is the ground truth value.

The MSE data is useful to find the best results that fit the correct model. Gradient descent is an optimization method for computing a local minimum of a function based on MSE data. The latter method iterates the results in the opposite direction of the gradient until a minimum is computed (Fig. 6) [26].

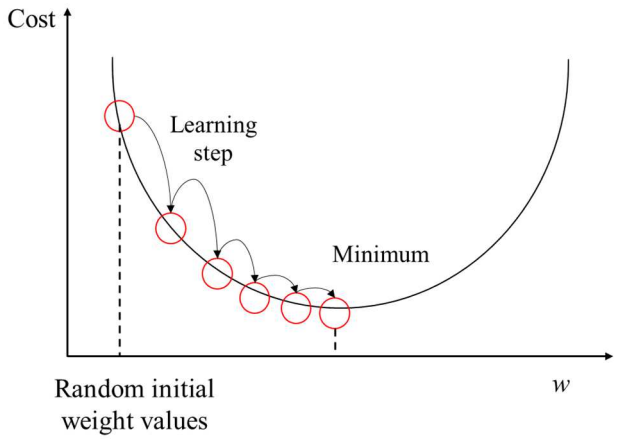

Fig. 6: Gradient descent model. The red circles indicate the local minimum after each iteration.

The Gradient Descent algorithm is described in Fig. 7. The algorithm was programmed in Python 3.0 based on the Keras and TensorFlow libraries [27,28].

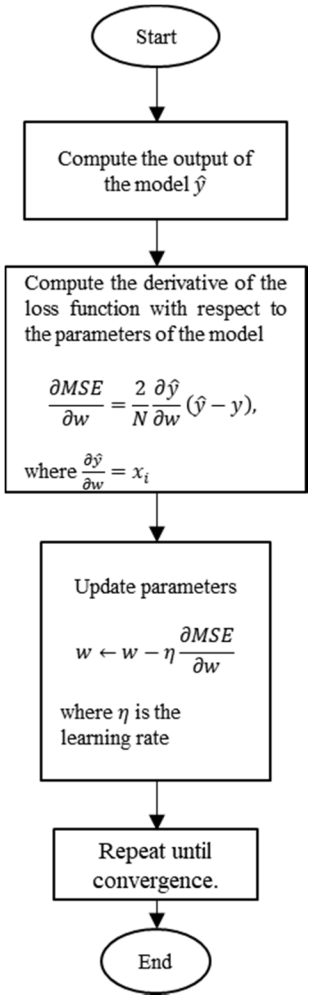

Fig. 7: Gradient descent algorithm flow chart.

D. Validation

The validation was performed by comparing the radiometric database and temperature matrices taken at the feet of 15 volunteers presented in [29]. The volunteer selection conditions neither considered age, gender, or background of DM, nor visible alterations on the foot, since the objective at this stage is to characterize the Lepton sensor to the thermal camera. Each volunteer was placed with the bare feet as steady as possible. The feet rested over support as depicted in Fig. 8. The thermal camera was placed 92 cm regard the soul of the feet, while the Lepton sensor was placed at 40 cm, which is the recommended focal distance to obtain full-frame capture of the object of interest.

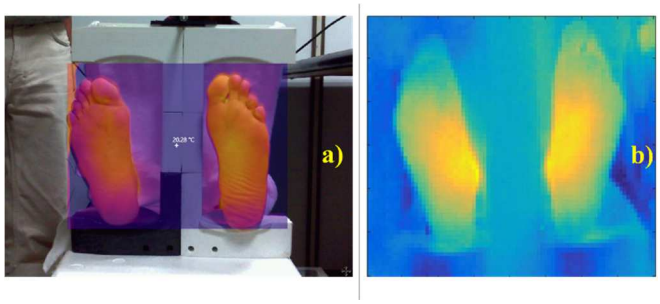

Fig. 8: Volunteer samples IR images. a) False color image sample taken with the Ti32 thermal camera, b) IR image reconstructed with radiometric data of the Lepton Sensor.

The temperature differences were computed comparing the temperature matrices obtained between the Ti32 thermal camera and both regression models, reported in [15] and the one obtained with the Perceptron method.

III. Results

The optimized weight and bias calculated with the Perceptron and Gradient Descent method is presented in equation 4 with an R = 0.99.

$$y(x) = 0.044x - 323.73 \quad (4)$$

The last MSE value retrieved after the optimization step was 0.0203 with an initial weight $w = 0.01$ (see Fig. 9).

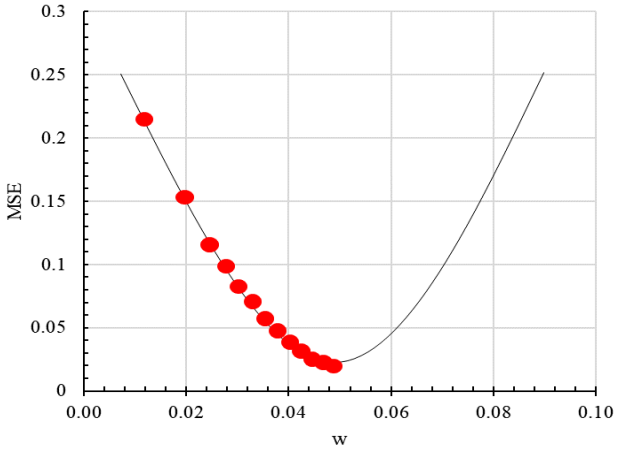

Fig. 9: Gradient Descent algorithm updates the weights of the model in the direction that minimizes the loss function.

Once the model was optimized, the equation was applied to the Lepton radiometric arrays to retrieve a temperature matrix that describes the superficial temperature measured. The data were compared in 9 specific points where the feet can prone to loss of sensation according to the filament examination, depicted in Fig. 10 [30].

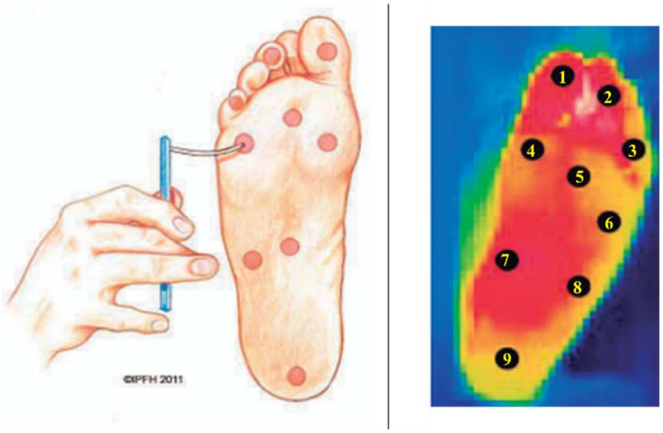

Fig. 10: Common zones for developing ulcers, according to the filament examination for diabetic foot detection.

Fig. 11 and Fig. 12 presents the absolute error computed between average values of the first regression model (equation 5) vs. the Ti32 and the ANN model vs. the Ti32. The temperature values were retrieved from 36 temperature arrays. Table 2 resumes the average error for both sets, as the standard deviation.

$$y = 1 \times 10^{-5}x^2 + 0.2604x - 1157.7 \qquad (5)$$

Table 2: Comparison between the linear regression model and the Perceptron optimized model.

	Original model	Perceptron linear regression
Average absolute error [°C]	1.28	0.14
Standard deviation	0.27	0.02

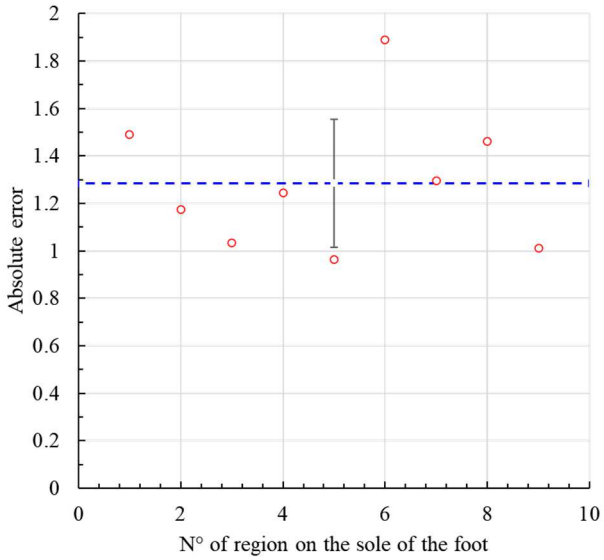

Fig. 11: Absolute error for the first regression model in [15]. The blue line represents the absolute average error (error μ = 1.28°C) while the vertical line represents the standard deviation (σ = 0.27).

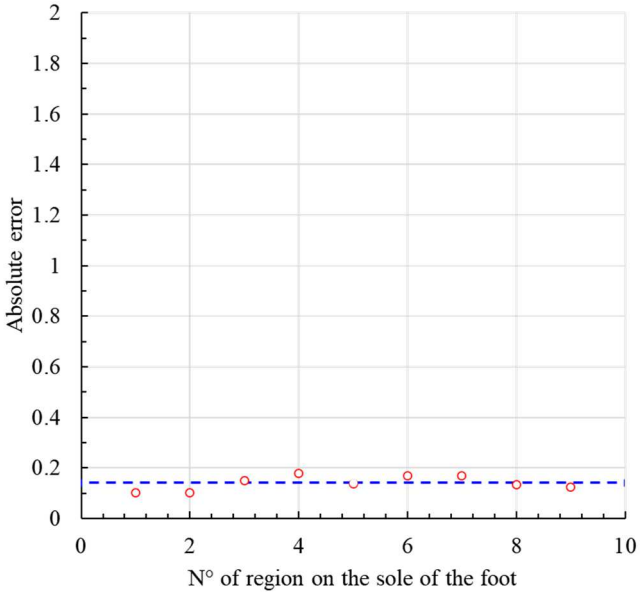

Fig. 12: Absolute error for the Perceptron linear regression. The blue line represents the absolute average error (error μ = 0.14°C). The standard deviation is imperceptible due to the scale standardization (σ = 0.026).

IV. Discussion

The results proved to have a significantly less error than the mathematical model in [15] based on an ANN to obtain a linear regression The results obtained in this work could not only be due to regression with significantly more data (23 values vs. 948 values) but also due to a characterization under better-controlled conditions, involving robust temperature measurement equipment such as an industrial purpose thermal camera previously calibrated with a gold standard thermometer.

However, the optimization of the linear model with the Gradient Descent method contributed to have an absolute error of less than half a degree Celsius concerning the Ti32 equipment. Although this mathematical model does not improve the resolution of the measurements due to the intrinsic characteristics of the Lepton sensor, it can now provide more accurate measurements, especially since it has been used in several studies related to the diabetic foot to understand the physiological changes from a quantitative point of view [31,32].

It is expected that this paper contributes to quantitative thermography with portable embedded systems employing low-cost sensors and development kits; particularly, when the sensor has a linear response. Several works have addressed problems of medical thermography from nonlinear approaches, in which the use of ANN training is an optimal solution [16,33,34]. It is well-known that there are discussion groups and forums where a way to calibrate this type of technology for different purposes is being actively discussed [35]; particularly for our case is the early detection of diabetic foot studies.

V. Conclusions

A basic ANN (linear regression by Perceptron) training method was presented in this work to obtain a mathematical model. The model corresponds to an improvement of the characteristic equation previously described by Bayareh et al. in [15] for the Lepton 2.5 sensor to perform quantitative thermography studies in the early detection of diabetic foot. In this way, the sensor could retrieve radiometric information extracted in 14-bit values to predict temperatures maps in the Celsius scale, exclusively for skin surface temperature scanning. The linear model obtained in this work presented an average error decrease of 0.14°C concerning the Fluke Ti32 industrial-purpose thermal camera, while the original model had an average error of 1.28ºC.

Although the model obtained by the Perceptron method and optimized by Gradient Descent had a better performance than the original model, the characterization conditions were significantly improved concerning the first work. The new model could be used in the future to improve segmentation based on temperature difference, due to the improvement of the accuracy in a low-cost and portable LWIR radiometric sensor such as Lepton 2.5. The latter prototype was build in 2017 under a budget of $350 USD, which is a 85% cheaper than the model Ti32. As a perspective, the improvement of the resolution is contemplated with the implementation of the Lepton 3.5 sensor, the same sensor that has been used under the same objective in [36].

Acknowledgment

We appreciate the funding for the development of the work presented project: CYTED-DITECROD-218RT0545 and Proyecto IV-8 call Amexcid-Auci 2018-2020.

Special thanks to MSc. José Hugo Zepeda Peralta and MSc. Rubén Pérez Valladares for their collaboration and contribution in this work.

References

1. Cho, N.H. *IDF Diabetes Atlas Ninth edition 2019*; www.inisco.; 2019; ISBN 978-2-930229-87-4.
2. Pendsey, S.P. Understanding diabetic foot. *Int. J. Diabetes Dev. Ctries.* 2010.
3. Bharara, M.; Cobb, J.E.; Claremont, D.J. Thermography and thermometry in the assessment of diabetic neuropathic foot: A case for furthering the role of thermal techniques. *Int. J. Low. Extrem. Wounds* **2006**, *5*, 250–260, doi:10.1177/1534734606293481.
4. Jiao, F.F.; Cheung Fung, C.S.; Fai Wan, E.Y.; Chun Chan, A.K.; McGhee, S.M.; Ping Kwok, R.L.; Kuen Lam, C. Lo Five-Year cost-effectiveness of the multidisciplinary risk assessment and management programme–Diabetes mellitus (RAMP- DM). *Diabetes Care* **2018**, doi:10.2337/dc17-1149.
5. Lahiri, B.B.; Bagavathiappan, S.; Jayakumar, T.; Philip, J. Medical applications of infrared thermography: A review. *Infrared Phys. Technol.* **2012**, *55*, 221–235, doi:10.1016/j.infrared.2012.03.007.
6. Diakides, N.A.; Diakides, M.; Lupo, J.; Paul, J.L.; Balcerak, R. Advances in medical infrared imaging. In *Medical Devices and Systems*; CRC Press, 2006; pp. 19-1-19–14 ISBN 9781420003864.
7. Kaczmarek, M.; Nowakowski, A. Active IR-Thermal Imaging in Medicine. *J. Nondestruct. Eval.* **2016**, *35*, 1–16, doi:10.1007/s10921-016-0335-y.
8. Wijlens, A.M.; Holloway, S.; Bus, S.A.; van Netten, J.J. An explorative study on the validity of various definitions of a 2·2°C temperature threshold as warning signal for impending diabetic foot ulceration. *Int. Wound J.* **2017**, doi:10.1111/iwj.12811.
9. Bernard, V.; Staffa, E.; Mornstein, V.; Bourek, A. Infrared camera assessment of skin surface temperature - Effect of emissivity. *Phys. Medica* **2013**, *29*, 583–591, doi:10.1016/j.ejmp.2012.09.003.
10. Liu, C.; van Netten, J.J.; van Baal, J.G.; Bus, S.A.; van der Heijden, F. Automatic detection of diabetic foot complications with infrared thermography by asymmetric analysis. *J. Biomed. Opt.* **2015**, *20*, 026003, doi:10.1117/1.jbo.20.2.026003.
11. Bayareh, R.; Vera, A.; Leija, L.; Gutierrez-Martínez, J. Development of a thermographic image instrument using the raspberry Pi embedded system for the study of the diabetic foot. *I2MTC 2018 - 2018 IEEE Int. Instrum. Meas. Technol. Conf. Discov. New Horizons Instrum. Meas. Proc.* **2018**, 1–6, doi:10.1109/I2MTC.2018.8409841.

12. Borchartt, T.B.; Conci, A.; Lima, R.C.F.; Resmini, R.; Sanchez, A. Breast thermography from an image processing viewpoint - A survey. **2013**, *93*, 2785–2803.

13. Modest, F.M. *Radiative Heat Transfer*; Press, A., Ed.; 2nd ed.; California, 2003;

14. Steketee, J. Spectral emissivity of skin and pericardium. *Phys. Med. Biol.* **1973**, *18*, doi:10.1088/0031-9155/18/5/307.

15. Bayareh-Mancilla, R.; Vera-Hernández, A.; Leija-Salas, L.; Ramos, A.; Gutierrez-Martínez, J. Characterization of a Longwave infrared imager for the telemetric measurement of human skin temperature of diabetic foot. In Proceedings of the Pan American Health Care Exchanges, PAHCE; 2017; Vol. 2017-March, pp. 70–74.

16. Muniz, P.R.; Cani, S.P.N.; Da S. Magalhaes, R. Influence of field of view of thermal imagers and angle of view on temperature measurements by infrared thermovision. *IEEE Sens. J.* **2014**, *14*, 729–733, doi:10.1109/JSEN.2013.2287003.

17. Cheng, T.Y.; Deng, D.; Herman, C. Curvature effect quantification for in-vivo IR thermography. In Proceedings of the ASME International Mechanical Engineering Congress and Exposition, Proceedings (IMECE); American Society of Mechanical Engineers, 2012; Vol. 2, pp. 127–133.

18. López, F.; Nicolau, V. Multivariate Infrared Signal Processing by Partial Least-Squares Thermography.

19. Barshan, E.; Ghodsi, A.; Azimifar, Z.; Zolghadri Jahromi, M. Supervised principal component analysis: Visualization, classification and regression on subspaces and submanifolds. *Pattern Recognit.* **2011**, *44*, 1357–1371, doi:10.1016/J.PATCOG.2010.12.015.

20. Bayareh Mancilla, R.; Tán, B.; Daul, C.; Gutiérrez Martínez, J.; Leija Salas, L.; Wolf, D.; Vera Hernández, A. Anatomical 3D Modeling Using IR Sensors and Radiometric Processing Based on Structure from Motion: Towards a Tool for the Diabetic Foot Diagnosis. *Sensors* **2021**, *21*, 3918, doi:10.3390/s21113918.

21. Beauducel, F. READIS2: Import IS2 files (Fluke infrared camera) Available online: https://www.mathworks.com/matlabcentral/%0Afileexchange/32352-readis2-import-is2-files-fluke-infrared-camera (accessed on Dec 10, 2019).

22. Bayareh, R.; Vera, A.; Leija, L.; Gutierrez-Martinez, J. Programming of a system for the acquisition of images and thermographic data for the diabetic foot analysis. *2017 14th Int. Conf. Electr. Eng. Comput. Sci. Autom. Control. CCE 2017* **2017**, 2–8, doi:10.1109/ICEEE.2017.8108866.

23. da Silva, I.N. *Artificial Neural Networks: A Practice Course*; 1st ed.; Springer Publishing Company, 2016; ISBN 3319431617.

24. Marsland, S. *Machine learning: An algorithmic perspective*; 2014;

25. Rosenblatt, F. Perceptron Simulation Experiments. *Proc. IRE* **1960**, *48*, doi:10.1109/JRPROC.1960.287598.

26. Strutz, T. *Data Fitting and Uncertainty: A practical introduction to weighted least squares and beyond*; 2011; ISBN 978-3-658-11455-8.

27. CHOLLET, F. *Deep Learning with Python, Manning*; 2018;

28. Abadi, M.; Barham, P.; Chen, J.; Chen, Z.; Davis, A.; Dean, J.; Devin, M.; Ghemawat, S.; Irving, G.; Isard, M.; et al. TensorFlow: A system for large-scale machine learning. In Proceedings of the Proceedings of the 12th USENIX Symposium on Operating Systems Design and Implementation, OSDI 2016; 2016.

29. Bayareh, R.; Maldonado, H.; Torres, I.A.; Vera, A.; Leija, L. Thermographic study of the diabetic foot of patients with diabetes mellitus and healthy patients. *2018 Glob. Med. Eng. Phys. Exch. Am. Heal. Care Exch. GMEPE/PAHCE 2018* **2018**, 1–5, doi:10.1109/GMEPE-PAHCE.2018.8400742.

30. Health Institute for preventive diabetic foot Neuropathy / Numbness Available online: https://www.ipfh.org/foot-conditions/foot-conditions-a-z/neuropathy-numbness.

31. Bayareh Mancilla, R.; Daul, C.; Gutierrez-Martínez, J.; Vera Hernández, A.; Wolf, D.; Leija Salas, L. Detection of Sore-risk Regions on the Foot Sole with Digital Image Processing and Passive Thermography in Diabetic Patients. *17th Int. Conf. Electr. Eng. Comput. Sci. Autom. Control* **2020**.

32. Bayareh Mancilla, R.; Daul, C.; Martinez, J.G.; Salas, L.L.; Wolf, D.; Hernandez, A.V. A Quantitative Method for the Detection of Temperature Differences on the Sole of the Foot in Diabetic Patients. In Proceedings of the Pan American Health Care Exchanges, PAHCE; IEEE, 2021; Vol. 2021-May, pp. 1–5.

33. Watmough, D.J.; Fowler, P.W.; Oliver, R. The thermal scanning of a curved isothermal surface: Implications for clinical thermography. *Phys. Med. Biol.* **1970**, *15*, 1–8, doi:10.1088/0031-9155/15/1/301.

34. Oxide, V.; Silicon, A.; Titanate, B.S. Uncooled detectors for thermal imaging cameras Uncooled detectors : a brief history. *Read* **1970**.

35. Flir Lepton - Grupos de Google Available online: https://groups.google.com/g/flir-lepton?pli=1 (accessed on Jul 1, 2021).

36. Fraiwan, L.; AlKhodari, M.; Ninan, J.; Mustafa, B.; Saleh, A.; Ghazal, M. Diabetic foot ulcer mobile detection system using smart phone thermal camera: A feasibility study. *Biomed. Eng. Online* **2017**, *16*, 1–19, doi:10.1186/s12938-017-0408-x.